Archives of Biochemistry and Biophysics
Vol. 392, No. 2, August 15, pp. 311–320, 2001
doi:10.1006/abbi.2001.2464, available online at http://www.idealibrary.com on IDEAL®

Vanadate-Induced Cell Growth Regulation and the Role of Reactive Oxygen Species

Zhuo Zhang,*,† Chuanshu Huang,* Jingxia Li,* Stephen S. Leonard,* Robert Lanciotti,* Leon Butterworth,* and Xianglin Shi*,†,[1]

Health Effects Laboratory Division, National Institute for Occupational Safety and Health, Morgantown, West Virginia 26505; and †Department of Basic Pharmaceutical Sciences, West Virginia University, Morgantown, West Virginia 26506

Received March 30, 2001, and in revised form May 29, 2001; published online July 17, 2001

While vanadium compounds are known as potent toxicants as well as carcinogens, the mechanisms of their toxic and carcinogenic actions remain to be investigated. It is believed that an improper cell growth regulation leads to cancer development. The present study examines the effects of vanadate on cell cycle control and involvement of reactive oxygen species (ROS) in these vanadate-mediated responses in a human lung epithelial cell line, A549. Under vanadate stimulation, A549 cells generated hydroxyl radical (·OH), as determined by electron spin resonance (ESR), and hydrogen peroxide (H_2O_2) and superoxide anion ($O_2^{\cdot-}$), as detected by flow cytometry using specific dyes. The mechanism of ROS generation involved the reduction of molecular oxygen to $O_2^{\cdot-}$ by both a flavoenzyme-containing NADPH complex and the mitochondria electron transport chain. The $O_2^{\cdot-}$ in turn generated H_2O_2, which reacted with vanadium(IV) to generate ·OH radical through a Fenton-type reaction ($V(IV) + H_2O_2 \rightarrow V(V) + {\cdot}OH + OH^-$). The ROS generated by vanadate induced G_2/M phase arrest in a time- and dose-dependent manner as determined by measuring DNA content. Vanadate also increased p21 and Chk1 levels and reduced Cdc25C expression, leading to phosphorylation of Cdc2 and a slight increase in cyclin B_1 expression as analyzed by Western blot. Catalase, a specific antioxidant for H_2O_2, decreased vanadate-induced expression of p21 and Chk1, reduced phosphorylation of $Cdc2^{Tyr15}$, and decreased cyclin B_1 levels. Superoxide dismutase, a scavenger of $O_2^{\cdot-}$, or sodium formate, an inhibitor of ·OH, had no significant effects. The results obtained from the present study demonstrate that among ROS, H_2O_2 is the species responsible for vanadate-induced G_2/M phase arrest. Several regulatory pathways are involved: (1) activation of p21, (2) an increase of Chk1 expression and inhibition of Cdc25C, which results in phosphorylation of Cdc2 and possible inactivation of cyclin B_1/Cdc2 complex.

Key Words: **vanadate; cell cycle; reactive oxygen species; p21; Chk1; Cdc25C; Cdc2; cyclin B_1.**

Vanadium is widespread in the environment and is a trace metal in biological systems. It exists in water, rocks, and soil in low concentrations and in coal and oil deposits in relatively high concentrations. Vanadium is widely found in mining, steel, and steel-alloy making and in the chemical industry. In the periodic table, vanadium belongs to the first transition series and can form compounds in valences III, IV, and V. The vanadium(III) species are unstable at physiological pH and in the presence of oxygen. Vanadium(IV) is easily oxidized to vanadium(V) under physiological conditions and vanadium(V) species are found as vanadate anions. Workers occupationally exposed to vanadium are at risk as respirable particulates may penetrate deep into the pulmonary tract. Epidemiological studies have shown a correlation between vanadium exposure and the incidence of lung cancer in humans (1, 2). While the mechanisms of vanadium's toxicity and carcinogenicity remain to be investigated, it has been reported that this metal is able to regulate growth-factor-mediated signal transduction pathways, promote cell transformation, exert inhibitory effect on certain enzymatic systems, and decrease cell adhesion (3–5). Vanadium compounds were also reported to cause direct DNA damage such as strand breaks and hydroxylation of dG residues (6).

The ability of cells to maintain genomic integrity is vital for cell survival and proliferation. Lack of fidelity

[1] To whom correspondence should be addressed. Fax: (304) 285-5938. E-mail: xas0@cdc.gov.

0003-9861/01 $35.00

in DNA replication and maintenance can result in deleterious mutations leading to cell death or, in multicellular organisms, cancer (7). Signal transduction pathways play a key role in the regulation of cell cycle progression and stabilization of DNA under genotoxic stress. Cell-cycle checkpoints control the onset of DNA replication and mitosis in order to ensure the integrity of the genome (8, 9). Earlier studies have shown that sodium vanadate causes G_2/M arrest and Rb hypophosphorylation in T98 glioma cells (10), demonstrating that the G_2/M arrest induced by a peroxovanadium compound was related to the reduced activity of $p34^{cdc2}$ and inhibition of Cdc25C (11). A 2-h exposure of the melanoma cells to sodium vanadate led to the decrease of cyclin D (12). Other studies have indicated that the mitogenesis induced by vanadate in CSV3-1 cells was associated with the induction of the expression of protooncogenes, c-*jun* and *jun* B, two major components of the AP-1 transcription factor (13).

It has been reported that under oxidative stress, cycling cells will exhibit cell cycle checkpoint response (14, 15). It has been demonstrated that vanadate-mediated generation of reactive oxygen species (ROS)[2] plays an important role in its adverse biological effects (16, 17). A recent study has also shown that vanadate induces apoptosis via hydrogen peroxide (H_2O_2) (18). However, many questions remain to be answered concerning the role of ROS in cell growth regulation in general and in vanadate-stimulated cells in particular. For example, (a) Are ROS involved in vanadate-induced cell growth arrest and cell cycle regulatory checkpoints? (b) Among the ROS, which species is directly responsible? (c) What is the mechanism of ROS generation in vanadate-stimulated cells? The goal of this study was to answer these questions.

MATERIALS AND METHODS

Reagents. Sodium metavanadate was from Aldrich (Milwaukee, WI). RNase A, superoxide dismutase (SOD), sodium formate, catalase, diphenylene iodonium (DPI), and rotenone were from Sigma (St. Louis, MO). Propidium iodide (PI), 2′,7′-dichlorofluorescin diacetate (DCFH-DA) and dihydroethidium (HE) were from Molecular Probes (Eugene, OR). Both F12K nutrient mixture medium and fetal bovine serum (FBS) were purchased from Gibco BRL (Life Technologies, Gaithersburg, MD). Antibodies to p21, cyclin B_1, and Cdc25C were from Santa Cruz Biotechnology (Santa Cruz, CA). Phospho-$Cdc2^{Tyr15}$ and second AP linked anti-rabbit IgG were from Cell Signaling (Beverly, MA).

Cell culture. The human lung epithelial cell line, A549, was cultured in F12k nutrient mixture medium containing 10% FBS, 2 mM L-glutamine, and 25 μg/ml gentamicin in an incubator at 5% CO_2 and 37°C.

Treatments. For the time-course study, the cells were treated with 100 μM vanadate for 6, 12, 24, and 48 h. For the dose–response study, the cells were treated with 10, 25, 50, 100, and 200 μM vanadate for 24 h. For antioxidant inhibitory studies, SOD, sodium formate, or catalase was added 0.5 h prior to the vanadate treatment.

Measurement of cell cycle/DNA content. DNA content in G_1/S, G_2/M phase was analyzed using flow cytometry (19, 20). Cells were first fixed and permeabilized with 70% ice-cold ethanol for more than 2 h, followed by incubation with the freshly prepared staining buffer (0.1% Triton X-100 in PBS, 200 μg/ml RNase A, and 20 μg/ml PI) for 15 min at 37°C. Cell cycle analysis was performed by flow cytometry with at least 10,000 cells for each sample. The histogram was abstracted and the percentage of cells in the G_1/S and G_2/M phase was then calculated using ModFit LT software.

Western blot analysis. Whole-cell extracts were mixed with SDS–polyacrylamide sample buffer and then subjected to SDS–polyacrylamide gel electrophoresis. The resolved proteins were transferred to a PVDF membrane. A Western blot assay was performed using antibodies against p21, Cdc25C, cyclin B_1, and phospho-$Cdc2^{Tyr15}$ and second anti-rabbit IgG. After reaction with ECF substrate, the signal was detected using a Storm Scanner (Molecular Dynamics, Sunnyvale, CA).

Electron spin resonance (ESR) measurements. ESR spin trapping was used to examine free radical generation. This technique involves an addition-type reaction of a short-lived radical with a diamagnetic compound (spin trap) to form a relatively long-lived free radical product, the so-called spin adduct, which can be studied by conventional ESR (21). The intensity of the spin adduct signal corresponds to the amount of short-lived radicals trapped, and the hyperfine splittings of the spin adduct are generally characteristic of the original, short-lived, trapped radical.

All measurements were conducted using a Varian E9 ESR spectrometer and a flat cell assembly as described previously (17). Briefly, hyperfine couplings were measured directly from magnetic field separation using potassium tetraperoxochromate (K_3CrO_8) and 1,1-diphenyl-2-picrylhydrazyl (DPPH) as reference standards. The relative radical concentration was calculated by multiplying half of the peak height by $(\Delta H_{pp})^2$, which indicates peak-to-peak width. A549 cells were mixed with DMPO to a total final volume of 0.5 ml. The reaction mixture was transferred to a flat cell for measurement.

Cellular hydrogen peroxide (H_2O_2) and superoxide anion ($O_2^{\cdot -}$) assay. DCFH-DA is a specific molecular probe for H_2O_2, and HE is a specific dye for $O_2^{\cdot -}$. The principle of this assay is that DCFH-DA diffuses through the cell membrane and is enzymatically hydrolyzed by intracellular esterases to nonfluorescent dichlorofluorescin (DCFH). In the presence of H_2O_2, this compound is rapidly oxidized to highly fluorescent dichlorofluorescein (DCF) (22, 23). HE is oxidized to ethidium that stains nucleus a bright fluorescent red (24). A549 cells were cultured in six-well plates. Each well contained 5×10^5 cells. The cells were treated with 100 μM vanadate for 1 h. DCFH-DA and HE (final concentration, 5 μM) were added to the cells and incubated for another 15–20 min prior to measurement of fluorescence. The harvested cells were washed with PBS twice. The samples were analyzed using flow cytometry.

Oxygen consumption assay. The reaction mixtures contained 1×10^6/ml cells and 100 μM vanadate. Oxygen consumption was determined using a Gilson oxygraph equipped with a Clark electrode. The oxygraph was calibrated with medium equilibrated with oxygen of known concentrations.

Statistical analysis. All data were based on at least three independent experiments. Cell growth arrest and oxygen consumption data were presented as means ± SD and analyzed using one-way

[2] Abbreviations used: ROS, reactive oxygen species; SOD, superoxide dismutase; DPI, diphenylene iodonium; PI, propidium iodide; DCFH-DA, 2′,7′-dichlorofluorescin diacetate. HE, dihydroethidium; FBS, fetal bovine serum; PBS, phosphate-buffered saline; PVDF, polyvinylidene fluoride; DPPH; 1,1,-diphenyl-2-polyhydroxyl; DMPO, 5,5-dimethyl-1-pirroline-*N*-oxide; DCFH, dichlorofluorescin; DCF, dichlorofluorescein; MPF, mitosis-promoting factor; ECF, enzyme catalytic fluorescence.

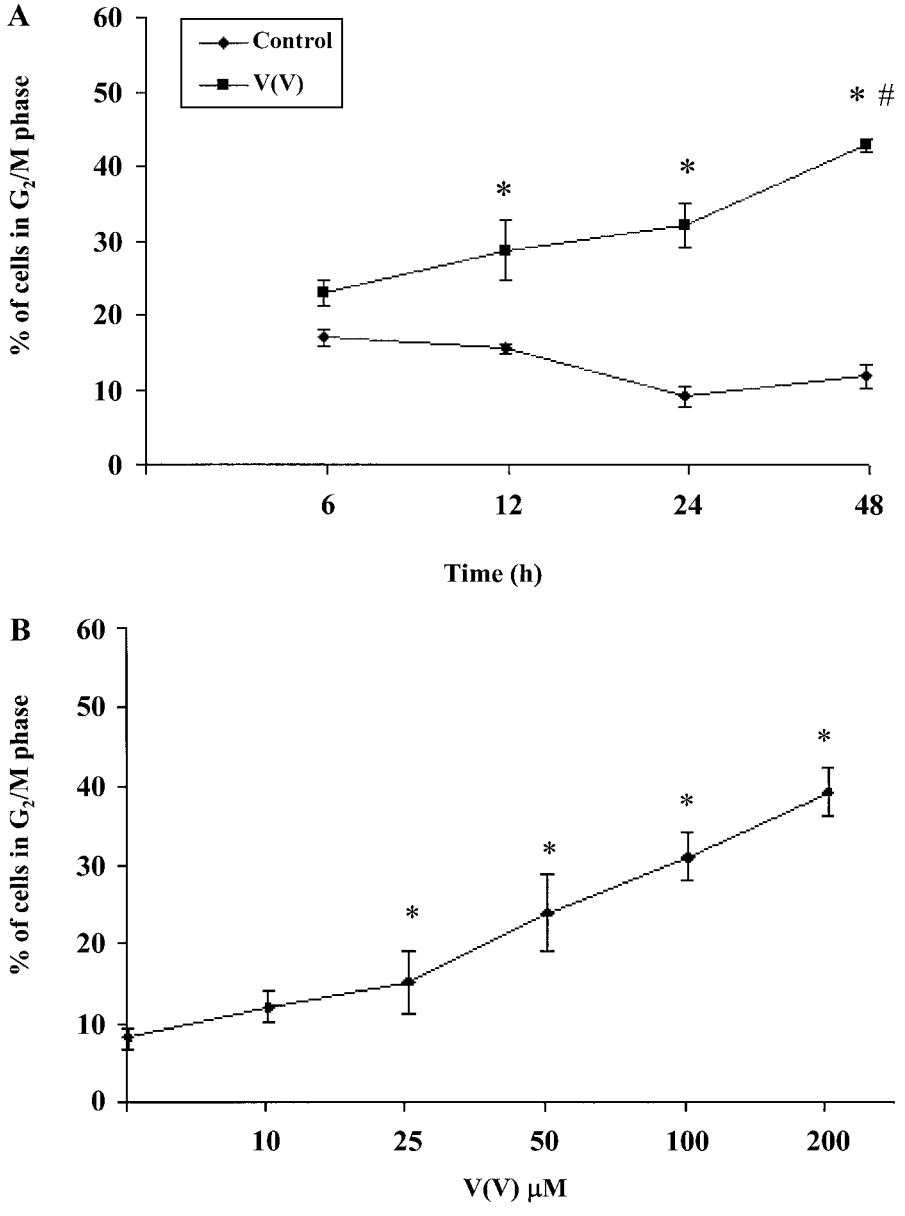

FIG. 1. Vanadate-induced cell growth arrest. A549 cells were suspended in 10% fetal bovine serum (FBS) F12 K nutrient mixture medium in a 100-mm dish. After 80–90% confluence, cells were washed with PBS for three times and treated with 100 μM vanadate for 6, 12, 24, and 48 h (A) or with 10, 25, 50, 100 μM vanadate for 24 h (B). Cells were harvested and DNA content was measured by flow cytometry. *$P < 0.05$ compared to control. #$P < 0.05$ compared to 6 h vanadate treatment (one-way ANOVA with Scheffe's test).

ANOVA with the Scheffe's test. A P value less than 0.05 was considered statistically significant.

RESULTS

Effects of vanadate on the cell cycle. To investigate vanadate-induced cell growth arrest, DNA content was measured by flow cytometry. Figure 1A shows that treatment of A549 cells with 100 μM vanadate causes a significant increase in the percentage of cells in G_2/M phase from 12 h onward. The percentage of cells in G_2/M phase in the control cells remains at a constant level from 6 to 48 h of incubation. Figure 1B shows the dose-dependent increase in the percentage of cells in G_2/M phase when the cells were treated with vanadate for 24 h. At 100 μM vanadate, the percentage of cells in G_2/M phase was fourfold greater than control value.

Effects of vanadate on cell growth regulatory proteins. Cell growth regulatory proteins were examined by Western blotting. The treatment of cells with vanadate caused a time- and dose-dependent increase in

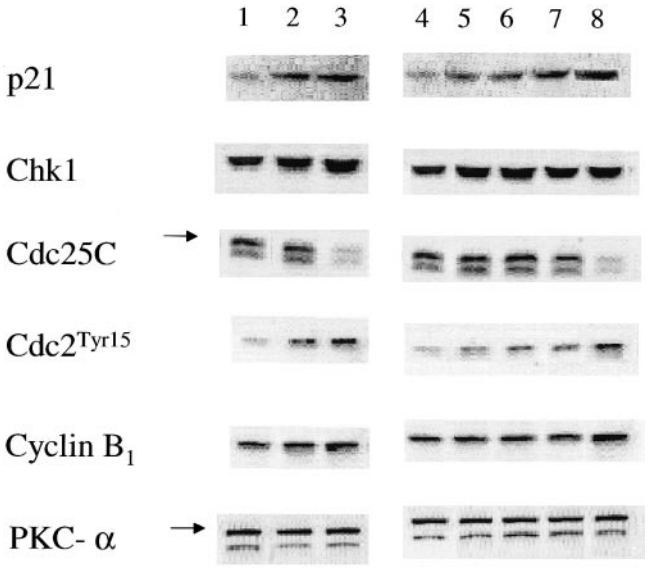

FIG. 2. Effects of vanadate on cell growth regulatory proteins. Cells were cultured in a six-well plate until 80–90% confluent. After washing with PBS three times, cells were treated with 100 μM vanadate for different times and different concentrations of vanadate for 24 h as described in Fig. 1. The whole cell lysates were collected for Western blotting using specific antibodies to p21, Chk1, Cdc25C, phospho-Cdc2^{Tyr15}, cyclin B_1, and PKC-α (as a control of loaded protein). (Left) Time dependence. Lane 1, control without vanadate; lane 2, 12 h; lane 3, 24 h. The concentration of vanadate was 100 μM. (Right) Concentration dependence. Lane 4, control without vanadate; lane 5, 10 μM vanadate; lane 6, 25 μM vanadate; lane 7, 50 μM vanadate; lane 8, 100 μM vanadate. The incubation time was 24 h.

p21 level (Fig. 2). The level of Chk1 increased with 100 μM vanadate stimulation. Using the 24-h time point, increased Chk1 levels were seen at vanadate concentrations from 10 to 100 μM. Treatment of cells with 100 μM vanadate for 24 h caused degradation in Cdc25C (Fig. 2). Cdc25B level did not exhibit any change (data not shown). As expected, both phosphorylation of Cdc2^{Tyr15} and cyclin B_1 level increased compared to the control. The PKC-α protein was used as a control for loaded protein.

Effects of antioxidants on vanadate-induced cell growth arrest. Figure 3 shows the different effects of antioxidants on vanadate-induced G_2/M phase arrest. The percentage of G_2/M phase exhibited little change after treatment of the cells with SOD, formate or catalase without vanadate present (data not shown). SOD, formate, and catalase are scavengers for superoxide radical ($O_2^{\cdot -}$), hydroxyl radical (·OH), and H_2O_2, respectively. The cells were incubated with these individual antioxidants together with 100 μM vanadate for 24 h. Vanadate significantly increased the percentage of cells in G_2/M phase. Both SOD and formate had no significant effect on this vanadate-induced G_2/M phase arrest. Treatment with catalase decreased G_2/M phase arrest induced by vanadate.

Effects of antioxidants on vanadate-regulated cell growth checkpoints. Figure 4 shows that treatment of the cells with catalase decreases both p21 and Chk1 levels induced by vanadate (100 μM), resulting in a reduction of both Cdc2^{Tyr15} and cyclin B_1. Catalase appeared to enhance vanadate-induced Cdc25C degrada-

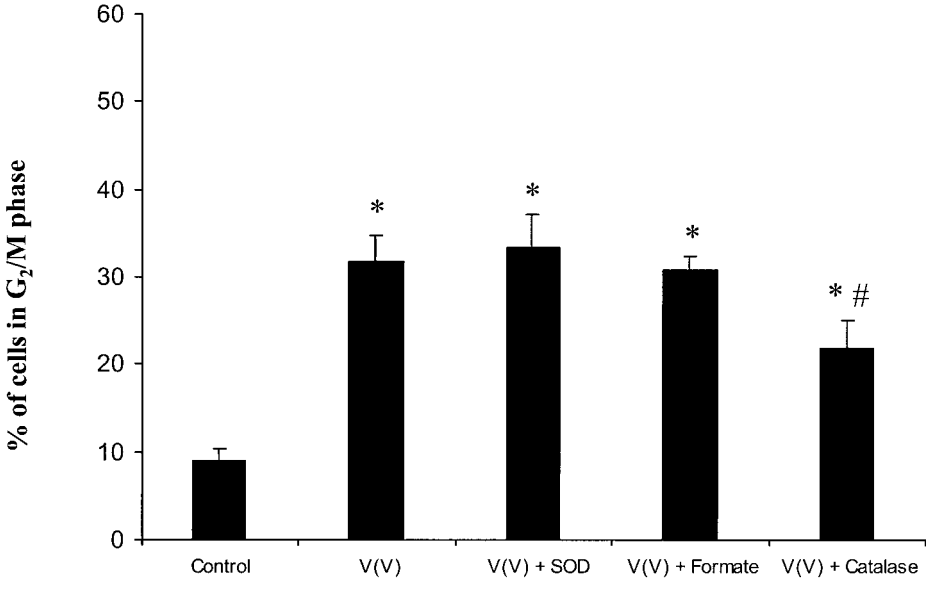

FIG. 3. Effects of antioxidants on vanadate-induced cell growth arrest. A549 cells were incubated in a 100-mm dish and pretreated with 500 U/ml SOD, 300 μM sodium formate or 50,000 U/ml catalase for 0.5 h before vanadate treatment (100 μM). After 24 h, cells were harvested, and DNA content was measured by flow cytometry. *$P < 0.05$ compared to control. #$P < 0.05$ compared to vanadate treatment (one-way ANOVA with the Scheffe's test).

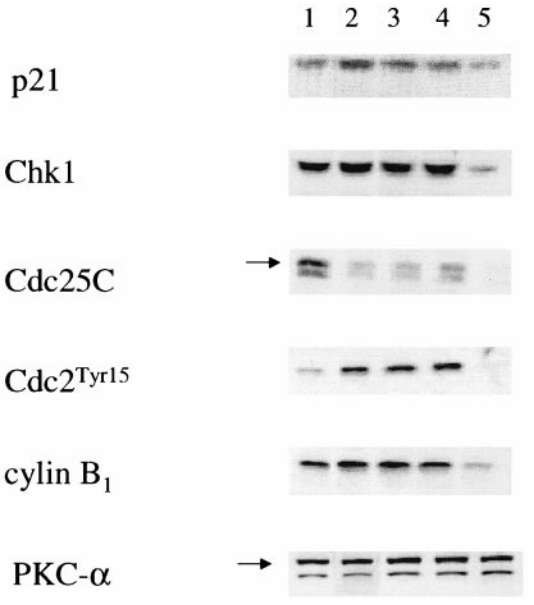

FIG. 4. Effects of antioxidants on vanadate-regulated cell growth checkpoints. Cells were seeded in a six-well plate and pretreated with SOD, sodium formate, or catalase for 0.5 h before vanadate treatment (100 μM). After 24 h, cells were collected for Western blotting using specific antibodies to p21, Chk1, Cdc25C, phospho-Cdc2^{Tyr15}, cyclin B_1, and PKC-α (as control of loaded protein). Lane 1, control; lane 2, vanadate; lane 3, vanadate + SOD; lane 4, vanadate + sodium formate; lane 5, vanadate + catalase. The results are representative of three separate experiments.

tion. Treatment with SOD (500 U/ml) or formate (300 μM) slightly decreased Cdc25C degradation by vanadate and had little effect on p21 and Chk1. Neither SOD nor formate changed Cdc2^{Tyr15} or cyclin B_1 level.

Hydroxyl radical formation induced by vanadate and the effects of antioxidants. ESR study was used to detect the formation of ·OH. A549 cells alone did not produce any detectable amount of free radicals (Fig. 5a), whereas addition of 100 μM vanadate generated a 1:2:2:1 quartet ESR spin adduct signal (Fig. 5b). The splittings of this spectrum were $a_H = a_N = 14.9$ G, where a_H and a_N denote hyperfine splittings of the α-hydrogen and the nitroxyl nitrogen, respectively, indicating the DMPO-OH adduct. The detection of this DMPO-OH spin adduct is evidence for ·OH generation. Addition of formate, an ·OH scavenger, significantly reduced the signal intensity (Fig. 5c). Catalase, a specific scavenger of H_2O_2, eliminated the generation of ·OH (Fig. 5d). The inhibition of ·OH generation upon addition of catalase indicates that H_2O_2 was generated and that it was a precursor for ·OH generation. It is possible that NADPH oxidase or the mitochondrial electron transport chain or both play a major role in this vanadate-induced ROS generation. In order to investigate this possibility, DPI and rotenone were used. DPI and rotenone were reported to be an NADPH oxidase inhibitor and a mitochondrial electron transport interrupter (25). The results show that both DPI and rotenone reduced ·OH generation induced by vanadate (Figs. 5e and 5f). Moreover, the spin adduct signal was completely eliminated upon addition of DPI and rotenone together (Fig. 5g), indicating that both NADPH oxidase and the mitochondria electron transport chain were responsible for vanadate-induced ROS generation.

Formation of hydrogen peroxide and superoxide anion radical induced by vanadate and the effects of antioxidants. As shown in Fig. 6, the generation of H_2O_2 and $O_2^{\cdot-}$ was determined using dye staining. Compared to control, treatment of cells with 100 μM vanadate for 1 h increased H_2O_2 formation by 75% (Fig. 6A). Since dye staining is not specific for the detection of H_2O_2 or $O_2^{\cdot-}$, specific antioxidants, catalase, and SOD were used to verify that these species were indeed detected. Catalase inhibited vanadate-induced H_2O_2 formation by 70%. Only a slight change was observed after treatment of the cells with SOD or formate, i.e., a decrease of 8 or 17%, respectively. Figure 6B shows that 100 μM vanadate dramatically increased $O_2^{\cdot-}$ formation by 63%. SOD, a specific scavenger of $O_2^{\cdot-}$, reduced vana-

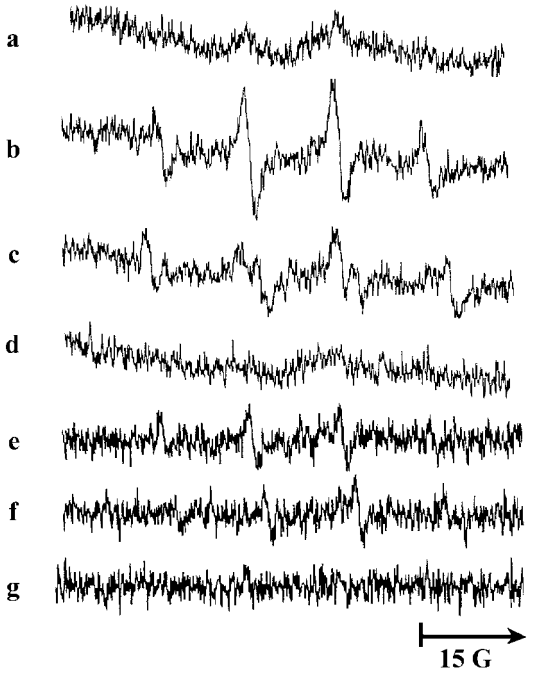

FIG. 5. Hydroxyl radical formation induced by vanadate and the effects of antioxidants. 1×10^6 cells were mixtured with 100 mM DMPO and 100 μM vanadate with or without antioxidants, DPI, or rotenone. ESR spectra were recorded for 6 min. a, Cells only; b, cells + vanadate; c, cells + vanadate + sodium formate; d, cells + vanadate + catalase; e, cells + vanadate + DPI; f, cells + vanadate + rotenone; g, cells + vanadate + DPI + rotenone. The final concentrations were as follows: vanadate, 100 μM; catalase, 2000 U/ml; sodium formate, 100 mM; DPI, 20 μM; rotenone, 50 μM.

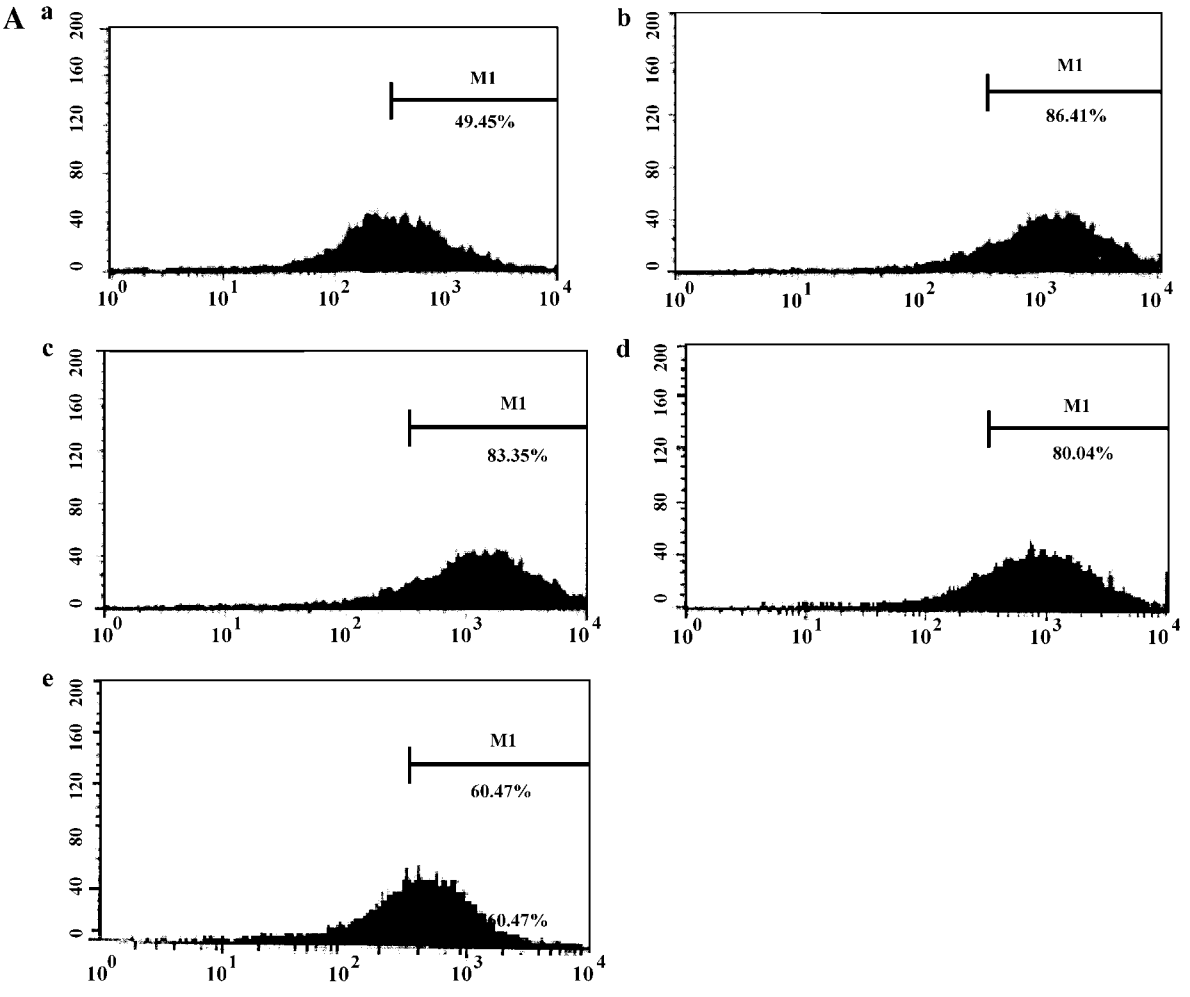

FIG. 6. Formation of H_2O_2 and $O_2^{\cdot-}$ induced by vanadate and the effects of antioxidants. Cells were cultured in a 6-well plate. After 80–90% confluence, cells were treated with 100 μM vanadate for 1 h. For evaluation of antioxidant effects, the cells were pretreated with 500 U/ml SOD, 300 mM formate, or 5000 U/ml catalase for 0.5 h before 100 μM vanadate treatment. DCFH-DA or HE was added to the cells and incubated for another 15–20 min at 37°C. Then the cells were washed with PBS twice and collected for analysis using flow cytometry. A and B represent H_2O_2 and $O_2^{\cdot-}$ signals, respectively. a, Control; b, vanadate; c, vanadate + SOD; d, vanadate + sodium formate; e, vanadate + catalase.

date-induced $O_2^{\cdot-}$ formation by 97%. Formate or catalase had smaller effects on vanadate-induced $O_2^{\cdot-}$ formation, i.e., a decrease of 22 or 10%, respectively. As $O_2^{\cdot-}$ is the one-electron reduction product of molecular oxygen, the O_2 consumption from cells was measured using an oxygraph. O_2 consumption was 1600 nmol/10^6 cells after vanadate treatment, whereas it was 1200 nmol/10^6 cells in controls; i.e., vanadate significantly increased O_2 consumption by 33% (Fig. 7).

DISCUSSION

Damage to growing cells causes a temporary pause in G_1/S or G_2/M phase until the damage is repaired. When damage is severe, cells may either undergo apoptosis or enter a dormant G_0 state. Regulation of cell cycle progression is achieved by events including cyclin accumulation and degradation; phosphorylations of Cdks, cyclins, and other proteins; regulation of cyclin/Cdk dimerization; and the binding of a number of Cdk inhibitory proteins (24–28). Movement of cells from $G_2 \rightarrow$ M is regulated by cyclin A and cyclin B/Cdc2. Cyclin B/Cdc2 kinase activity peaks in late G_2 and remains high until its degradation (29). This kinase has been identified as being a principal component of mitosis promoting factor (MPF) (30). In mammalian cells, three cyclin B isoforms have been characterized: cyclin B_1, cyclin B_2, and cyclin B_3. Cyclin B_1 plays an important role in maintaining G_2/M transition and its progression (31). The present study shows that vanadate induces G_2/M phase arrest in both a time- and a dose-dependent manner. G_2/M phase arrest increased after treatment with 100 μM vanadate for 6 h

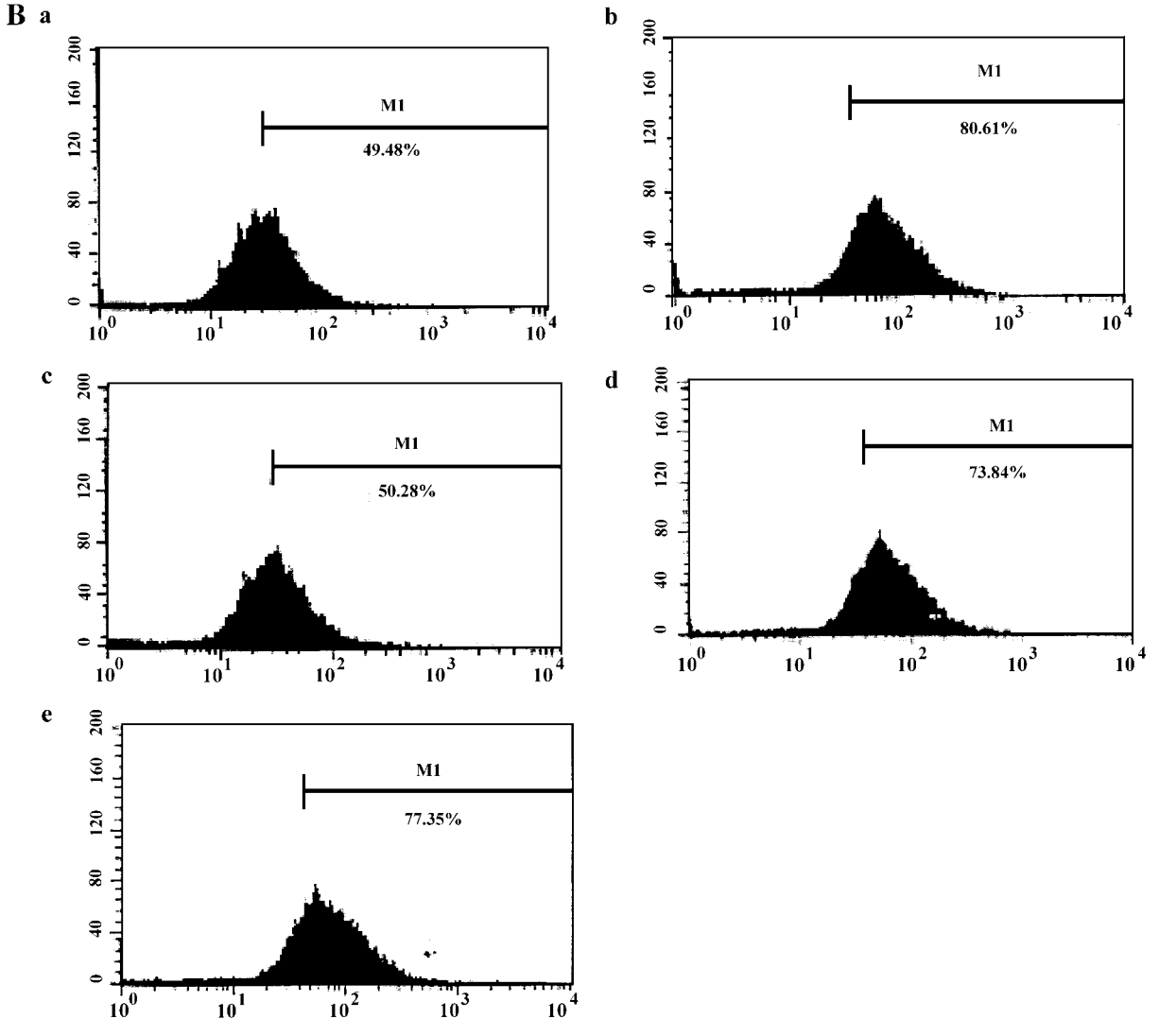

FIG. 6—*Continued*

and was maintained at a high level through 48 h. The percentage of cells in G_2/M phase significantly increased when cells were treated with 25 μM vanadate for 24 h. A549 cells treated with 400 μM vanadate for 24 h underwent apoptosis (data not shown).

Cell cycle checkpoints monitor movement through the cell cycle, survey for cell damage, and induce a pause in cell cycle progression when necessary. There are two pathways associated with cyclin B/Cdc2 complex: (a) Cdc25C phosphatase activates cyclin B/Cdc2 by dephosphorylated Thr-14/Tyr-15 (32), and this association between Cdc25C and cyclin B/Cdc2 complex may be blocked through the actions of the Chk1 and Chk2 kinases which phosphorylate Cdc25C on serine 216 (33). This phosphorylation is necessary for binding to 14-3-3 proteins and its apparent sequestration from the cyclin B/Cdc2 complex (34–36). (b) Transcriptional activation of $p21^{WAF1/CIP1}$ binds to and inactivates cyclin B/Cdc2 complex that is required for the cell cycle progression (37–39). γ-Irradiation results in an accumulation of Thr-14/Tyr-15 phosphorylated Cdc2, leading to inhibition of cyclin B/Cdc2 activity (40, 41). Our results show that vanadate was able to activate Chk1, resulting in degradation of Cdc25C, which could not remove $Cdc2^{Tyr15}$ phosphorylation. This may result in inactivation of the cyclin B_1/Cdc2 complex. Further, our results show that vanadate increased the level of p21 in a time- and dose-dependent manner. Induction of p21 inhibits cell progression in two ways: (a) by inhibiting a variety of cyclin/cdk complexes and (b) by inhibiting DNA synthesis through PCNA binding (42). The p53 protein activates transcription of the p21 gene (43–45), although activation of p21 can also be p53 independent (46, 47). The results from our previous study also demonstrate that vanadate indeed increased p53 protein level (data not shown), resulting in activation of p21.

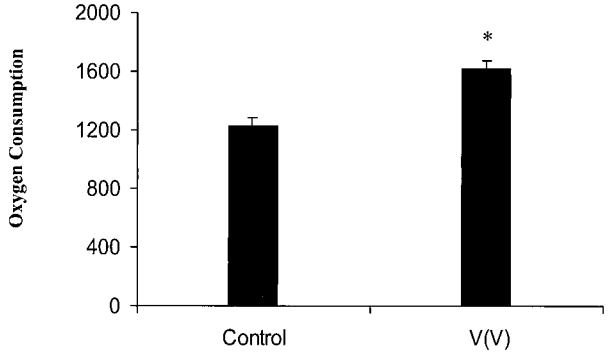

FIG. 7. Measurement of oxygen consumption. 1×10^6 Cells were prepared for detection of oxygen consumption using oxygraph. The final concentration of vanadate was 100 μM. $^*P < 0.05$ compared to control (one-way ANOVA with Scheffe's test).

Both p53 and p21 levels decrease after pretreated with Pifithrin-α, a specific inhibitor of p53 in both JB6 cells and fibroblasts (48). These results indicate that activation of p21 induced by vanadate is p53-dependent.

The accumulation of ROS-induced cellular damage is believed to be an important cause of various pathological processes, including aging, cancer, diabetes mellitus, atherosclerosis, and neurological degeneration (49–51). ROS are capable of damaging many cellular components including DNA (52). DNA damage results in the activation of mechanisms that arrest cell cycle progression at specific checkpoints, presumably to allow time for the damage to be repaired (14). Under oxidative stress, cycling cells will exhibit a cell cycle checkpoint response (14, 15). The results from the present study show that under vanadate stimulation, A549 cells are able to generate $O_2^{\cdot -}$, H_2O_2, and ·OH radicals. Molecular oxygen is the original source of ROS generation in vanadate-stimulated A549 cells as demonstrated by the oxygen consumption assay. The major pathways involved are both the flavoprotein-containing NADPH oxidase complex and the mitochondrial electron transport chain. This conclusion was supported by the inhibition of ROS generation by DPI, a flavoprotein inhibitor, as well as rotenone, an inhibitor of the mitochondrial electron transport chain. Molecular oxygen was consumed to generate $O_2^{\cdot -}$, which produced H_2O_2 upon dismutation. H_2O_2 produced ·OH via a Fenton-like reaction (V(IV) + $H_2O_2 \rightarrow$ V(V) + ·OH + OH^-). Catalase scavenged H_2O_2, a precursor of ·OH, and inhibited ·OH generation.

Among ROS generated by vanadate-stimulation of A549 cells, H_2O_2 appears to be the species responsible for vanadate-induced cell growth arrest at the G_2/M phase. The following experimental observations support this conclusion: (a) Catalase, a specific H_2O_2 scavenger, decreased vanadate-induced growth arrest. (b) Neither SOD, a $O_2^{\cdot -}$ scavenger, nor sodium formate, an ·OH radical scavenger, exhibited any effect. Both catalase and SOD are efficient H_2O_2 and $O_2^{\cdot -}$ scavengers. Using confocal microscope together with specific fluorescent dyes, we have shown that addition of catalase or SOD extracellularly reduced H_2O_2 or $O_2^{\cdot -}$ generated inside the A549 cells under Cr(VI) stimulation to control level (24, 53). Using flow cytometry, we have shown in the present study that catalase reduced vanadate-induced H_2O_2 formation by 70%.

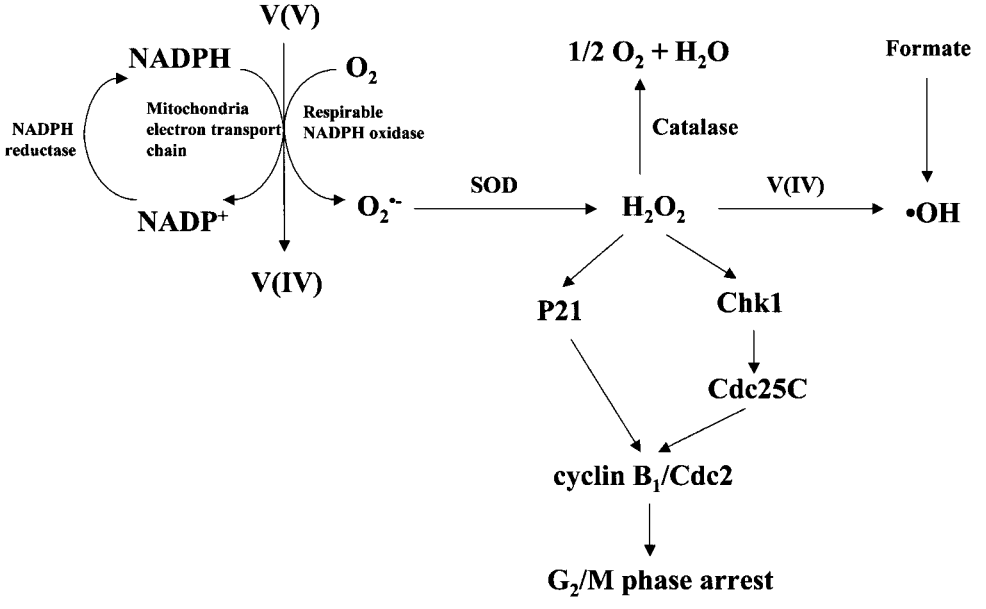

FIG. 8. Schematic representation of possible mechanisms of vanadate (V)-induced cell growth arrest and its regulation via generation of H_2O_2 in A549 cells.

In addition to the identification of the role of H_2O_2 in vanadate-induced cell growth arrest at the G_2/M phase, the present study also examined the regulatory enzymes involved. The results obtained show that among ROS generated by vanadate-stimulated cells, H_2O_2 is the species responsible for an increase in p21 and Chk1, $Cdc2^{Tyr15}$, and cyclin B_1 as demonstrated by inhibition with catalase. It may be noted catalase did not protect vanadate-induced Cdc25C degradation, indicating that H_2O_2 is not a major species responsible for vanadate-induced Cdc25C degradation. Neither SOD nor formate exhibited a major effect on these regulatory enzymes. A scheme for vanadate-induced ROS generation, its induction of cell growth arrest at the G_2/M phase, and its effect on cell growth-related regulatory enzymes is illustrated in Fig. 8. It should be noted that earlier studies (54–56) have shown that Wee1 and Mik1 kinase can also phosphorylate cdc2 and regulate its activity. It is possible that this mechanism together those discussed in the present study all contribute to the vanadate-induced cell growth arrest at G_2/M phase and its regulation.

In summary, vanadate is able to induce G_2/M phase arrest through ROS-mediated reactions. Among ROS generated by vanadate-stimulated A549 cells, H_2O_2 is the species responsible for vanadate-induced cell growth arrest and the regulation of several key enzymes involved. The H_2O_2 was generated by dismutation of $O_2^{\cdot -}$. The latter was produced by one-electron reduction of molecular oxygen by both NADPH reductase and the mitochondria electron transport chain.

REFERENCES

1. Stock, P. (1960) On the relations between atmospheric pollution in urban and rural localities and mortality from cancer, bronchitis, pneumonia, with particular reference t0 3,4-benzopyrene, beryllium, molybdenum, vanadium and arsenic. *Br. J. Cancer* **14,** 397–418.
2. Hickey, R. J., Schoff, E. P., and Clelland, R. C. (1967) Relationship between air pollution and certain chronic disease death rates. *Arch. Environ. Health* **15,** 728–738.
3. Cruz, T. F., Morgan, A., and Min, W. (1995) In vitro and in vivo antineoplastic effects of orthovanadate. *Mol. Cell Biochem.* **153,** 161–166.
4. Swarup, G., Cohen, S., and Garbers, D. L. (1982) Inhibition of membrane phosphotyrosyl-protein phosphatase activity by vanadate. *Biochem. Biophys. Res. Commun.* **107,** 1104–1109.
5. Stern, A., Yin, X., Tsang, S. S., Davison, A., and Moon, J. (1993) Vanadium as a modulator of cellular regulatory cascades and oncogene expression. *Biochem. Cell Biol.* **71,** 103–112.
6. Shi, X., Jiang, H., Mao, Y., Ye, J., and Saffiotti, U. (1996) Vanadium(IV)-mediated free radical generation and related 2′-deoxyguanosine hydroxylation and DNA damage. *Toxicology* **106,** 27–38.
7. Shackelford, R. E., Kaufmann, W. K., and Paules, R. S. (1999) Cell cycle control, checkpoint mechanisms, and genotoxic stress. *Environ. Health Perspect.* **107**(Suppl. 1), 5–24.
8. Hartwell, L. H., and Kastan, M. B. (1994) Cell cycle control and cancer. *Science* **266,** 1821–1828.
9. Mercer, W. E. (1998) Checking on the cell cycle. *J. Cell. Biochem. Suppl.* **30/31,** 50–54.
10. Chin, L. S., Murray, S. F., Harter, D. H., Doherty, P. F., and Singh, S. K. (1999) Sodium vanadate inhibits apoptosis in malignant glioma cells: A role for Akt/PKB. *J. Biomed. Sci.* **6,** 213–218.
11. Faure, R., Vincent, M., Dufour, M., Shaver, A., and Posner, B. I. (1995) Arrest at the G_2/M transition of the cell cycle by protein-tyrosine phosphatase inhibition: Studies on a neuronal and a glial cell line. *J. Cell Biochem.* **58,** 389–401.
12. Strasberg, R. M., and Rieber, M. (1995) Suppression of cyclin D1 but not cdk4 or cyclin A with induction of melanoma terminal differentiation. *Biochem. Biophys. Res. Commun.* **216,** 422–427.
13. Wang, H., Xie, Z., and Scott, R. E. (1995) Induction of AP-1 activity associated with c-Jun and JunB is required for mitogenesis induced by insulin and vanadate in SV40-transformed 3T3T cells. *Mol. Cell Biochem.* **168,** 21–30.
14. Russo, T., Zambrano, N., Esposito, F., Ammendola, R., Cimino, F., Fiscella, M., Jackman, J., O'Connor, P. M., Anderson, C. W., and Appella, E. (1995) A p53-independent pathway for activation of WAF_1/CIP_1 expression following oxidative stress. *J. Biol. Chem.* **270,** 29,386–29,391.
15. Chen, Q. M., Bartholomew, J. C., Campisi, J., Acosta, M., Reagan, J. D., and Ames, B. N. (1998) Molecular analysis of H_2O_2-induced senescent-like growth arrest in normal human fibrosis: p53 and Rb control G_1 arrest but not cell replication. *Biochem. J.* **332,** 43–50.
16. Ye, J., Ding, M., Leonard, S. S., Robinson, V. A., Millecchia, L., Zhang, X., Castranova, V., Vallyathan, V., and Shi, X. (1999) Vanadate induces apoptosis in epidermal JB6 P+ cells via hydrogen peroxide-mediated reactions. *Mol. Cell Biochem.* **202,** 9–17.
17. Shi, X., and Dalal, N. S. (1992) Hydroxyl radical generation in the NADH/microsomal reduction of vanadate. *Free Radical Res. Commun.* **17,** 369–376.
18. Huang, C., Zhang, Z., Ding, M., Li, J., Ye, J., Leonard, S. S., Shen, H., Lu, Y., Castranova, V., Vallyathan, V., and Shi, X. (2000) Vanadate (V)-induced apoptosis through hydrogen peroxide-mediated p53 dependent pathway. *J. Biol. Chem.* **275,** 32,516–32,522.
19. Nicoletti, I., Migliorati, G., Pagliacci, M. C., Grignani, F., and Riccardi, C. (1991) A rapid and simple method for measuring thymocyte apoptosis by propidium iodide staining and flow cytometry. *J. Immunol. Methods* **139,** 271–279.
20. Sgonic, R., and Wick, G. (1994) Methods for the detection of apoptosis. *Int. Arch. Allergy Immunol.* **105,** 327–332.
21. Rosen, G. M., and Finkelstein, E. (1985) Use of spin traps in biological systems. *Adv. Free Radical Biol. Med.* **1,** 345–375.
22. Bass, D. A., Parce, J. W., Dechatelet, L. R., Szejda, P., Seeds, M. C., and Thomas, M. (1983) Flow cytometric studies of oxidative product formation by neutrophils: A graded response to membrane stimulation. *J. Immunol.* **130,** 1910–1917.
23. LeBel, C. P., Ischiopoulos, H., and Bondy, S. C. (1992) Evaluation of the probe 2′,7′-dichlorofluorescin as an indicator of reactive oxygen species formation and oxidative stress. *Chem. Res. Toxicol.* **5,** 227–231.
24. Ye, J., Wang, S., Leonard, S. S., Sun, Y., Butterworth, L., Antonini, J., Ding, M., Rojanasakul, Y., Vallyathan, V., Castranova, V., and Shi, X. (1999) Role of reactive oxygen species and p53 in chromium (VI)-induced apoptosis. *J. Biol. Chem.* **274,** 34,974–34,980.

25. Irani, K., Xia, Y., Zweier, J. L., Sollott, S. J., Der, C. J., Fearon, E. R., Sundaresan, M., Finkel, T., and Goldschmidt-Clermont, P. J. (1997) Mitogenic signaling mediated by oxidants in ras-transformed fibroblasts. *Science* **275,** 1649–1652.
26. Morgan, D. O. (1995) Principles of CDK regulation. *Nature* **374,** 131–134.
27. Draetta, G. (1990) Cell cycle control in eukaryotes: Molecular mechanisms of Cdc2 activation. *Trends Biochem. Sci.* **15,** 378–383.
28. Norbury, C., and Nurse, P. (1993) Animal cell cycles and their control. *Annu. Rev. Biochem.* **61,** 441–470.
29. Pines, J., and Hunter, T. (1989) Isolation of a human cyclin cDNA: Evidence for cyclin mRNA and protein regulation in the cell cycle and for interaction with $p34^{cdc2}$. *Cell* **58,** 833–846.
30. Arion, D., Meijer, L., Brizuela, L., and Beach, D. (1988) Cdc2 is a component of the M phase-specific histone H1 kinase: Evidence for identity with MPF. *Cell* **54,** 423–431.
31. Brandeis, M., Rosewell, I., Carrington, M., Crompton, T., Jacobs, M. A., Kirk, J., Gannon, J., and Hunt, T. (1998) Cyclin B2-null mice develop normally and are fertile whereas cyclin B1-null mice die in utero. *Proc. Natl. Acad. Sci. USA* **95,** 4344–4349.
32. Strausfeld, U., Labbe, J. C., Fesquet, D., Cavadore, J. C., Picard, A., Sadhu, K., Russell, P., and Doree, M. (1991) Dephosphorylation and activation of a p34 cdc2/cyclin B complex in vitro by human Cdc25 protein. *Nature* **351,** 242–245.
33. Shackelford, R. E., Kaufmann, W. K., and Paules, R. S. (2000) Oxidative stress and cell cycle checkpoint function. *Free Radical Biol. Med.* **28,** 1387–1404.
34. Peng, C. Y., Graves, P. R., Thoma, R. S., Wu, Z. Q., Shaw, A. S., and Piwnica-worms, H. (1997) Mitotic and G2 checkpoint control: Regulation of 14-3-3 protein binding by phosphorylation of Cdc25C on serine-216. *Science* **277,** 1501–1505.
35. Sanchez, Y., Wong, C., Thoma, R. S., Richman, R., Wu, R. Q., Piwnica-Worms, H., and Elledge, S. J. (1997) Conservation of the Chk1 checkpoint pathway in mammals: Linkage of DNA damage to Cdk regulation through Cdc25. *Science* **277,** 1497–1501.
36. Brown, A. L., Lee, C. H., Schwarz, J. K., Mitiku, N., Piwnica-Worms, H., and Chung, J. H. (1999) A human Cds1-related kinase that functions downstream of ATM protein in the cellular response to DNA damage. *Proc. Natl. Acad. Sci. USA* **96,** 3745–3750.
37. El-Deiry, W. S., Tokino, T., Velculescu, V. E., Levy, D. B., Parsons, R., Trent, J. M., Lin, D., Mercer, W. E., Kinzler, K. W., and Vogelstein, B. (1993) WAF1, a potential mediator of p53 tumor suppression. *Cell* **75,** 817–825.
38. Harper, J. W., Adami, G. R., Wei, N., Keyomarsi, K., and Elledge, S. J. (1993) The p21 cdk-interacting protein Cip_1 is a potent inhibitor of G_1 cyclin-dependent kinases. *Cell* **75,** 805–816.
39. Xiong, Y., Hannon, G. J., Zhang, H., Casso, D., Kobayashi, R., and Beach, D. (1993) p21 is a universal inhibitor of cyclin kinases. *Nature* **366,** 701–704.
40. Lock, R. B., and Ross, W. E. (1995) Inhibition of p34cdc2 kinase activity by etoposide or irradiation as a mechanism of G_2 arrest in Chinese hamster ovary cells. *Cancer Res.* **50,** 7–11.
41. Kaufmann, W. K., Levedakou, E. N., Grady, H. L., Paules, R. S., and Stein, G. H. (1995) Attenuation of G_2 checkpoint function precedes human cell immortalization. *Cancer Res.* **55,** 7–11.
42. Johnson, D. G., and Walker, C. L. (1999) Cyclins and cell cycle checkpoints. *Annu. Rev. Pharmacol. Toxicol.* **39,** 295–312.
43. Elledge, S. J., and Harper, J. W. (1994) Cdk inhibitors: On the threshold of checkpoints and development. *Curr. Opin. Cell Biol.* **6,** 847–852.
44. Sherr, C. J., and Roberts, J. M. (1995) Inhibitors of mammalian G1 cyclin-dependent kinases. *Genes Dev.* **9,** 1149–1163.
45. Bunz, F., Dutriaux, A., Lengauer, C., Waldman, T., Zhou, S., Brown, J. P., Sedivy, J. M., Kinzler, K. W., and Volelstein, B. (1998) Requirement for p53 and p21 to sustain G_2 arrest after DNA damage. *Science* **282,** 1497–1501.
46. Johnson, M., Dimitrov, D., Vojta, P. J., Barrett, J. C., Noda, A., Pereira, S. O., and Smith, J. R. (1994) Evidence for a p53-independent pathway for upregulation of SDI1/CIP1/WAF1/p21 RNA in human cells. *Mol. Carcinog.* **11,** 59–64.
47. Michieli, P., Chedid, M., Lin, D., Pierce, J. H., Mercer, W. E., and Givol, D. (1994) Induction of WAF1/CIP1 by a p53-independent pathway. *Cancer Res.* **54,** 3391–3395.
48. Zhang, Z., Huang, C., Li, J., and Shi, X. Vanadate-induced cell growth arrest is p53-dependent through activation of p21 in Cl41 cells. Submitted.
49. Floyd, R. A. (1990) Role of oxygen free radicals in carcinogenesis and brain ischemia. *FASEB J.* **4,** 2587–2597.
50. Ames, B. N., and Shigenaga, M. K. (1992) Oxidants are a major contributor to aging. *Ann. NY Acad. Sci.* **663,** 85–96.
51. Jenner, P. (1994) Oxidative damage in neurodegenerative disease. *Lancet* **344,** 796–798.
52. Payne, C. M., Bernsterin, C., and Bersterin, H. (1995) Apoptosis overview emphasizing the role of oxidative stress, DNA damage and signal-transduction pathways. *Leuk. Lymphoma.* **19,** 43–93.
53. Wang, S., Leonard, S. S., Ye, J., Ding, M., and Shi, X. (2000) The role of hydroxyl radical as a messenger in Cr(VI)-induced p53 activation. *Am. J. Physiol.* **279,** C868–C875.
54. Rhind, N., and Russell, P. (2000) Roles of the mitotic inhibitors Wee1 and Mik1 in the G(2) DNA damage and replication checkpoint. *Mol. Cell Biol.* **21,** 1499–1508.
55. Harrison, J. C., Bardes, E. S., Ohya, Y., and Lew, D. J. (2001) A role for Pkc1p/Mpk1p kinase cascade in the morphogenesis checkpoint. *Nat. Cell Biol.* **3,** 417–420.
56. Lee, J., Kumagai, A., and Dunphy, W. G. (2001) Positive regulation of Wee1 by chk1 and 14-3-3 proteins. *Mol. Biol. Cell* **12,** 551–563.